Retinoid X receptor ablation in adult mouse keratinocytes generates an atopic dermatitis triggered by thymic stromal lymphopoietin

Mei Li*, Nadia Messaddeq*, Marius Teletin†, Jean-Louis Pasquali‡, Daniel Metzger*†, and Pierre Chambon*†§¶

*Institut de Génétique et de Biologie Moléculaire et Cellulaire (IGBMC), †Institut Clinique de la Souris (ICS), §Collège de France, BP10142, 1, Rue Laurent Fries, Illkirch 67404, CU de Strasbourg, France; and ‡Laboratoire d'Immunopathologie, Hôpitaux Universitaires de Strasbourg, 1, Place de l'Hopital, 67000 Strasbourg, France

Contributed by Pierre Chambon, August 24, 2005

To investigate the role of retinoid X receptors (RXRs) in epidermal homeostasis, we generated RXR$\alpha\beta^{ep-/-}$ somatic mutants in which both RXRα and RXRβ are selectively ablated in epidermal keratinocytes of adult mice. These mice develop a chronic dermatitis mimicking that observed in atopic dermatitis (AD) patients. In addition, they exhibit immunological abnormalities including elevated serum levels of IgE and IgG, associated with blood and tissue eosinophilia, indicating that keratinocyte-selective ablation of RXRs also generates a systemic syndrome similar to that found in AD patients. Furthermore, the profile of increased expression of cytokines and chemokines in skin of keratinocyte-selective RXR$\alpha\beta$-ablated mutants was typical of a T helper 2-type inflammation, known to be crucially involved in human AD pathogenesis. Finally, we demonstrate that thymic stromal lymphopoietin, whose expression is rapidly and strongly induced in RXR$\alpha\beta$-ablated keratinocytes, plays a key role in initiating the skin and systemic AD-like pathologies.

keratinocyte-selective gene ablation | nuclear receptors | conditional mutagenesis | Cre-ER^{T2}

Atopic dermatitis (AD), a chronic skin inflammatory disease with a strong genetic component that affects children (10–20%) and adults (1–3%), is characterized by pruritic and eczematoid skin lesions, associated with systemic immunological abnormalities, including peripheral eosinophilia and hyper IgE immunoglobulinemia (1). Immunological mechanisms have been involved in AD pathogenesis (2), but the possible role of epidermal keratinocytes in AD initiation and maintenance is still largely unexplored (3).

Nuclear receptors (NRs) belong to a superfamily of transcriptional regulators that include ligand-dependent and orphan receptors (4, 5). NRs play critical roles as signal transducers in vertebrate development and homeostasis, including immune functions (4, 6–8). Within the NR superfamily, the retinoid X receptor isotypes (RXR α, β, and γ) play a key role as heterodimeric partners for some 15 NRs, e.g., retinoic acid receptors, 1,25-dihydroxyvitamin D_3 receptor (VDR), peroxisome proliferator-activated receptors, and liver X activated receptors (4, 5, 9). Ligand-dependent transcriptional activation by NRs requires the integrity of the core of activation function 2 (AF-2) (the α-helix 12 of the ligand-binding domain; see refs. 9 and 10).

In epidermis, RXRα is predominant, RXRβ level is lower, and RXRγ is undetectable (11–13). Keratinocyte-selective ablation of RXRα in adult mouse skin results in a number of abnormalities, including a progressive alopecia, keratinocyte hyperproliferation, and abnormal differentiation, and an inflammatory reaction (11, 14). In contrast, the skin of RXRβ-null mice is apparently normal (11, 14, 15).

To investigate the origin of this inflammatory reaction and to avoid any functional redundancies between keratinocytic RXRα and RXRβ, we have now generated RXR$\alpha\beta^{ep-/-}$ somatic mutants in which both RXRα and RXRβ are selectively ablated in epidermal keratinocytes of adult mice. These mice develop an AD-like chronic dermatitis, as well as a systemic syndrome, which share similarities with those found in AD patients. Thus, our data not only demonstrate that RXRs play a key role in the control of cutaneous inflammation, but also point to an initiating role of keratinocytes in AD. Moreover, we show that an early and strong enhancement of expression of the cytokine TSLP in RXR-ablated keratinocytes plays a crucial role in the generation of the AD-like skin and systemic syndrome.

Materials and Methods

Experimental Animals. RXR$\alpha\beta^{ep-/-}$ mice were obtained through tamoxifen (Tam) administration to K14-Cre-ER$^{T2(tg/0)}$/RXR$\alpha^{L2/L2}$/RXR$\beta^{L2/L2}$ adult mice, which harbor floxed RXRα and RXRβ L2 alleles and the K14-Cre-ER^{T2} transgene expressing the Tam-inducible Cre-ER^{T2} recombinase under the control of the keratin 14 (K14) promoter (11, 16, 17). Two weeks after Tam administration (week 2), recombined RXRα L$^-$ and RXRβ L$^-$ alleles were detected in skin, as well as in tongue, eyes and salivary glands (Fig. 7, which is published as supporting information on the PNAS web site). In RXR$\alpha\beta^{ep-/-}$ skin, the Cre-mediated conversion to L$^-$ alleles was restricted to the epidermis, where its efficiency was >90% (Fig. 7*b*). Tam-treated K14-Cre-ER$^{T2(0/0)}$/RXR$\alpha^{L2/L2}$/RXR$\beta^{L2/L2}$ and K14-Cre-ER$^{T2(tg/0)}$/RXR$\alpha^{L2/+}$/RXR$\beta^{L2/+}$ mice did not show any skin abnormalities, and were used as controls (CT). RXR$\alpha^{af2o/+}$ and RXR$\beta^{af2o/+}$ mouse lines have been described (18, 19). K14-TSLP transgenic mice are described in *Supporting Text*, which is published as supporting information on the PNAS web site.

Other Materials and Methods. Genotyping, Tam treatment, epidermal preparation, histopathology, immunohistochemistry, hematological assays, serum cytokine and immunoglobulin determination, RNA analysis and statistic analysis are all described in *Supporting Text*.

Results

Selective Ablation of RXRα and -β in Epidermal Keratinocytes of Adult Mice Leads to a Spontaneous Dermatitis. RXR$\alpha\beta^{ep-/-}$ mutants exhibited a progressive alopecia that became obvious by 6 weeks after Tam administration (week 6) to K14-Cre-ER$^{T2(tg/0)}$/RXR$\alpha^{L2/L2}$/RXR$\beta^{L2/L2}$ adult mice (see *Materials and Methods* and Fig. 7), and developed a spontaneous dermatitis that occurred predominantly on and behind the ears, on the face, in the neck region, and on the back (Fig. 1 *a–f*). At week 2, all mutant ears displayed reddening, swelling, and scaling (Fig. 1 *b* and *e*), whereas dry and scaly skin with small lesions became macroscopically visible

Abbreviations: AD, atopic dermatitis; AF-2, activation function 2; NR, nuclear receptor; RXR, retinoid X receptor; VDR, 1,25-dihydroxyvitamin D_3 receptor; Tam, tamoxifen; CT, control; DC, dendritic cell; Th, T helper; TSLP, thymic stromal lymphopoietin.

¶To whom correspondence should be addressed. E-mail: chambon@igbmc.u-strasbg.fr.

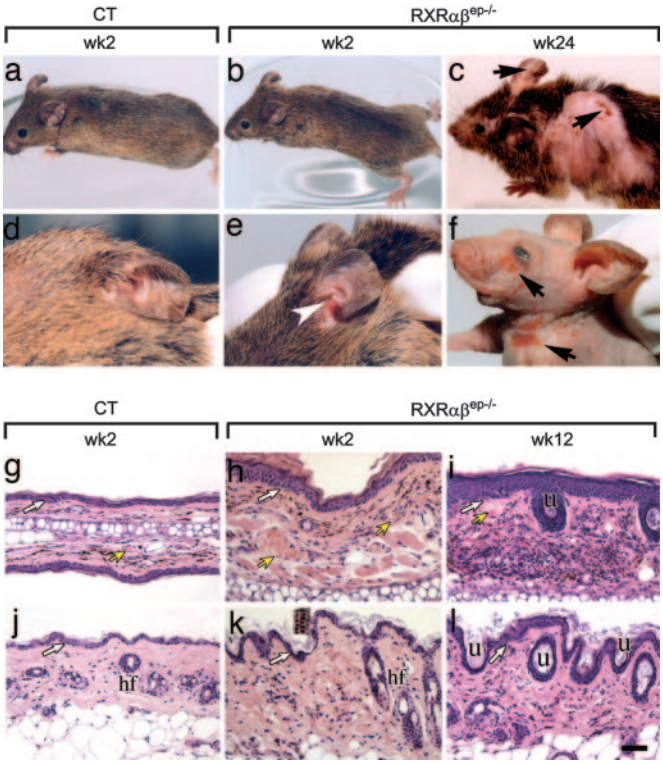

Fig. 1. RXR$\alpha\beta^{ep-/-}$ mice develop a chronic skin inflammation. (*a–f*) Appearance of control (CT) and RXR$\alpha\beta^{ep-/-}$ mutant mice at weeks 2 and 24 as indicated. The white arrowhead in *e* points to the reddening and thickening of a mutant ear at week 2, to be compared with its normal appearance in a CT mouse (*d*). Black arrows in *c* and *f* point to skin lesions seen at week 24 on the back and the ears, and on the face and the neck, respectively. (*g–l*) Hematoxylin and eosin-stained sections of ear (*g–i*) and dorsal skin (*j–l*) of CT and RXR$\alpha\beta^{ep-/-}$ mice at week 2 and week 12. White arrows point to dermal/epidermal junction. Yellow arrows point to blood vessels. hf, hair follicle; u, utriculi. (Scale bar, 50 μm.)

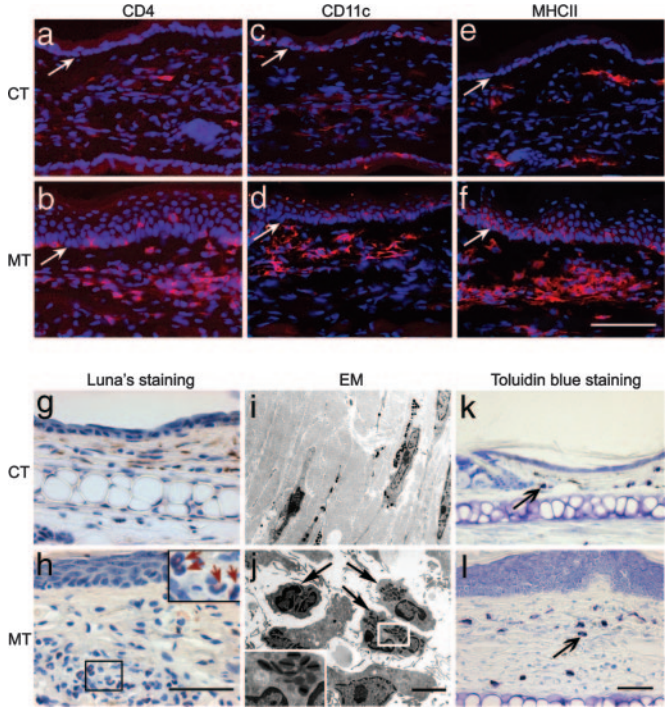

Fig. 2. Characterization of inflammatory cell infiltrates in ear skin. Immunohistochemical (IHC) staining was performed on ear sections from control (CT) and RXR$\alpha\beta^{ep-/-}$ mutant (MT) mice at week 8, with antibodies against CD4 (*a* and *b*), CD11c (*c* and *d*), and MHCII (*e* and *f*). Red color corresponds to staining of antibodies, whereas blue corresponds to DAPI staining of nuclei. White arrows point to dermal/epidermal junction. (Scale bar, 50 μm.) (*g* and *h*) Luna's staining. Eosinophils (pointed by red arrows in *h Inset*) display intracytoplasmic red staining. (*i* and *j*) Electron microscopic (EM) analyses. Eosinophils with crystal-like rectangular inclusions are pointed by black arrows and shown enlarged in *j Inset*. (*k* and *l*) Toluidin blue-stained sections. In each panel, the black arrow points to one of the mast cells showing intensive blue color. (Scale bars, 50 μm in *g*, *h*, *k*, and *l* and 2 μm in *i* and *j*.)

in the trunk at week 6-week 8 (not shown). The frequent face rubbing and scratching observed in these mutants most probably reflected a skin pruritus. The severity of these abnormalities worsened with age: by week 24, all mutants exhibited swollen and red ears, and 60% had developed ulcerations and crusts in the ear, neck, and back (Fig. 1 *c* and *f*). In contrast, RXR$\alpha^{ep-/-}$ mice developed only minor focal lesions on the dorsal skin at week 20 (11), whereas spontaneous dermatitis never occurred in RXR$\beta^{ep-/-}$ mice (not shown), clearly indicating a partial RXRα/RXRβ functional redundancy.

An Inflammatory Infiltrate in Skin of RXR$\alpha\beta^{ep-/-}$ Mice. At week 2, mutant ear (Fig. 1*h*) and to a lesser extent dorsal skin biopsies (Fig. 1*k*) revealed an epidermal hyperplasia, as well as infiltrated cells and dilated blood vessels in the dermis (compare with Fig. 1 *g* and *j*). At week 12, mutant ears exhibited a highly hyperplastic epidermis, together with a heavy dermal cell infiltrate (Fig. 1*i*), which was less dense in mutant dorsal skin (Fig. 1*l*). Bacterial or fungal infections were ruled out as possible causes of skin inflammation by Gram and periodic acid-schiff reagent staining and electron microscopy (not shown).

Immunohistochemistry staining for T lymphocytes performed on ear skin at week 8 revealed in RXR$\alpha\beta^{ep-/-}$ mutants numerous $CD4^+$ helper T cells, which were more abundant in the dermis than in the epidermis, whereas CT mice showed only few resident dermal $CD4^+$ cells (Fig. 2 *a* and *b* and data not shown). No $CD8^+$ T cell infiltrate was observed (not shown). CD11c, a marker for dendritic cells (DC), labeled resident epidermal Langerhans cells (LC) and few dermal DCs in CT (Fig. 2*c*), whereas in mutants, many DCs were revealed in the dermis, and the number of epidermal LCs was also increased (Fig. 2*d*). Staining with MHC class II antibody showed a strong increase in MHC II^+ cell number in mutant dermis (Fig. 2 *e* and *f*). MHC II expression was also detected in mutants, but not in CT keratinocytes, suggesting an "active" state for mutant keratinocytes. In addition, numerous eosinophils were revealed by Luna's staining (Fig. 2 *g* and *h*) and electron microscopy (Fig. 2 *i* and *j*) in mutant, but not in CT dermis. Mast cells were also more numerous in mutant dermis (Fig. 2 *k* and *l*), whereas neutrophils were rarely found in skin sections of both CT and mutants at week 8 (data not shown).

Analyses on mutant ear skin at week 2 showed that the appearance of $CD4^+$ T cell and DC infiltrate preceded the increase in eosinophils and mast cells. Furthermore, although less dense than in ear skin, similar cell infiltrates were also observed in mutant dorsal skin, involving $CD4^+$ T cells, DCs, eosinophils, and mast cells (Table 1, which is published as supporting information on the PNAS web site), thus evoking an immune cell pathological pattern characteristic of human AD (1, 20).

Preferential Expression of T Helper 2 (Th2)-Type Cytokines and Chemokines in RXR$\alpha\beta^{ep-/-}$ Skin. Because cytokines and chemokines orchestrate and determine the type and outcome of the inflammatory response, their relative RNA transcript level was determined by quantitative RT-PCR in CT and mutant ear skin from week 2 to week 12 (Fig. 3*a*). At weeks 4 and 12, analyses of cytokines

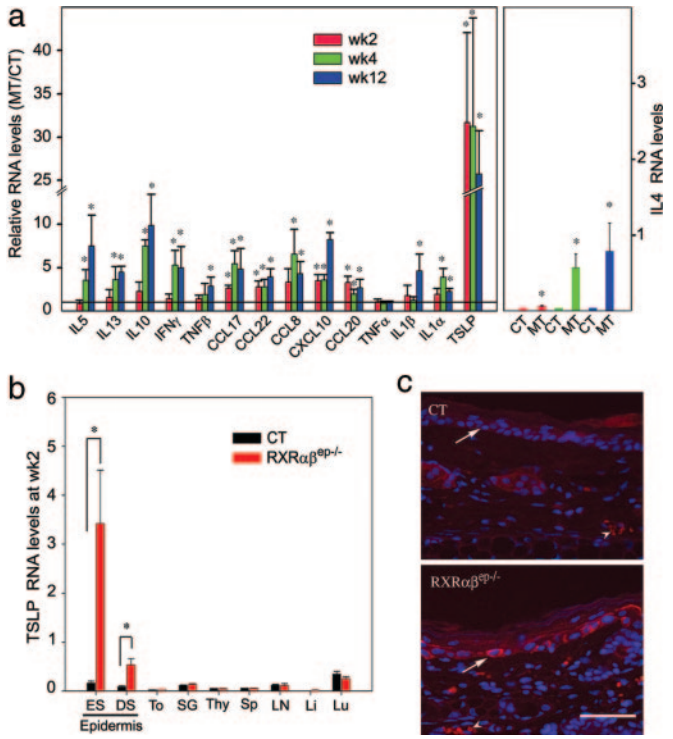

Fig. 3. Cytokine and chemokine expression in RXR$\alpha\beta^{ep-/-}$ skin. (*a*) Quantitative RT-PCR analyses of cytokines and chemokines in ear skin at week 2, week 4 and week 12. Relative expression levels in RXR$\alpha\beta^{ep-/-}$ mutants (MT) compared to controls (CT) (set as 1.0) are shown in *Left*; IL4 RNA levels of CT (undetectable at week 2–12) and MT are shown in *Right*. (*b*) TSLP RNA levels in epidermis of ear skin (ES) and dorsal skin (DS), tongue (To), salivary gland (SG), thymus (Thy), spleen (Sp), lymph node (LN), liver (Li), and lung (Lu) at week 2. *, $P < 0.05$. (*c*) Immunohistochemical staining of TSLP in ear skin at week 2. Red corresponds to antibody staining, and blue corresponds to DAPI staining of nuclei. White arrows point to dermal–epidermal junction. White arrowheads point to autofluorescence of erythrocytes. (Scale bar, 50 μm.)

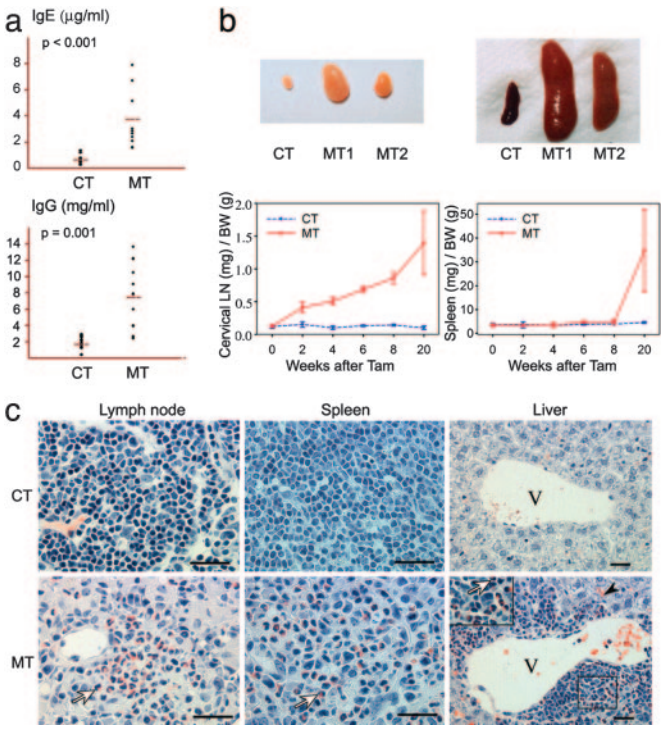

Fig. 4. Systemic immunological abnormalities in RXR$\alpha\beta^{ep-/-}$ mice. (*a*) IgE and IgG levels in sera of nine controls (CT) and nine mutant (MT) mice at week 12. The average values are indicated by short lines. (*b*) Lymph node (LN) hyperplasia and splenomegaly in MT mice. Cervical LNs and spleens from a CT and two MT mice (MT1 and MT2) are shown at week 20. The relative weights of cervical LN and spleen to body weights (BW) from CT and MT mice at week 0–20 are presented. (*c*) Luna's staining of cervical LN, spleen and liver sections (as indicated) at week 12. The white arrow points to one of the many eosinophils (stained red in cytoplasm and blue in nucleus). The black arrowhead points to erythrocytes (stained red in cytoplasm). V, vein. (Scale bar, 25 μm.)

produced by $CD4^+$ helper T cells (predominant in the RXR$\alpha\beta^{ep-/-}$ inflammatory infiltrate), revealed an increase of transcripts of Th2-type cytokines (21–23), including IL-5, IL-13, and IL-10, as well as IL-4, which was present in mutant skin, but could not be detected in CT skin. IL-31, a cytokine recently reported to be preferentially produced by Th2 cells (24), was also detected in mutant at week 4-week 12, but not in CT skin (data not shown, see also Fig. 5*h*). Transcripts of the Th1-type cytokine IFN-γ and TNF-β (21–23), were either similarly up-regulated at weeks 4 and 12 (IFN-γ) or only weakly at week 12 (TNF-β) (Fig. 3*a*).

Increased transcript levels of a number of chemokines (25, 26) were also found in mutant ear skin at week 2–12 (Fig. 3*a*), including (*i*) CCL17 (TARC) and CCL22 (MDC), chemoattractants for Th2 cells, (*ii*) CCL8 (MCP2), involved in recruitment of eosinophils and Th2 cells, (*iii*) CXCL10 (IP10, a chemoattractant for Th1 cells), and (*iv*) CCL20 (MIP3α, a chemoattractant for immature dendritic cells and Th1 cells). In contrast, RNA levels of chemokines CCL27, CCL5 (RANTES) and CCL11 (eotaxin) were unchanged (data not shown).

The RNA level of the proinflammatory cytokine TNF-α was not increased at any time in the mutants, whereas that of IL-1α was increased at weeks 4 and 12, and that of IL-1β was only increased at week 12 (Fig. 3*a*). Most interestingly, the transcript level of thymic stromal lymphopoietin (TSLP), a cytokine that was recently shown to be expressed at high levels in keratinocytes of AD patients and to instruct dendritic cells to preferentially induce a Th2 response *in vitro* (27), was strongly up-regulated (>15-fold) in mutant ear skin at weeks 2–12 (Fig. 3*a*). In contrast, the RNA level of IL-7, a cytokine functionally related to TSLP (28), was unchanged (not shown).

Early Enhancement of TSLP Expression in RXR$\alpha\beta^{ep-/-}$ Epidermal Keratinocytes. In ear skin (ES) at week 2, TSLP RNA levels were much higher in mutant than in control epidermis (Fig. 3*b*, ES; very little TSLP RNA was found in the dermis, not shown). Dorsal skin (DS) epidermis also showed an increased expression of TSLP, but to a lesser degree (Fig. 3*b*). TSLP transcript levels were unchanged in tongue and salivary glands in which ablation of RXRα and RXRβ was also detected (Fig. 7), and in other tissues including thymus, spleen, lymph node, liver, and lung (Fig. 3*b*, and data not shown).

An antibody against TSLP did not reveal its expression in either epidermis or dermis of CT ear skin at week 2, whereas it was readily detected in basal keratinocytes of mutant ear epidermis, but not in dermis (Fig. 3*c*), demonstrating that the expression of TSLP protein was strongly induced in RXR$\alpha\beta^{ep-/-}$ shortly after RXR$\alpha\beta$ ablation. In addition, TSLP serum levels were strongly increased as early as 1 week after this ablation (386 $\pm$ 138 pg/ml in mutant mice vs. <7.8 pg/ml in CT), and remained high (e.g., 449 $\pm$ 174 pg/ml at week 8) up to at least week 20 (data not shown).

Systemic Abnormalities in RXR$\alpha\beta^{ep-/-}$ Mice. At week 12, IgE and IgG levels were on average 5- and 4-fold higher in RXR$\alpha\beta^{ep-/-}$ mice than in CT, respectively, whereas IgM and IgA levels were unchanged (Fig. 4*a* and data not shown). IgG subtype IgG1, but not IgG2a, 2b, and 3, contributed to IgG increase (data not shown). IgE increased earlier than IgG, as a 3-fold increase of IgE was already

seen at week 4 in mutants, when no IgG elevation could be detected (data not shown). Further elevation of IgE and IgG1 levels was observed in RXR$\alpha\beta^{ep-/-}$ mice at week 20 (>20- and 10-fold higher than in CT, respectively, data not shown), suggesting a Th2-like systemic immune reaction (29).

Total white blood cell (WBC) counts at week 12 showed an average of 25,400 and 9,700 cells per μl in RXR$\alpha\beta^{ep-/-}$ mutants and CT, respectively. Eosinophil counts strikingly increased from 1.1% to 14.8% of total WBC, reaching an average of 3,760 cells per μl. Peripheral lymphocytes (19,600 cells per μl) and neutrophils (2,360 cells per μl) were also increased relative to CT (8,150 and 1,430 cells per μl, respectively).

At week 12 the serum concentration of IL-5, a critical factor for eosinophil expansion (30, 31), was much higher in RXR$\alpha\beta^{ep-/-}$ mutants (124 $\pm$ 19 pg/ml) than in CT (<16 pg/ml). IL-2, IL-4, IFN-γ, and TNF-α levels were too low to be detected in both CT and mutant sera (data not shown).

RXR$\alpha\beta^{ep-/-}$ mice exhibited hyperplasia of regional lymph nodes (LNs), which invariably included cervical LNs and, to a lesser extent, inguinal LNs (Fig. 4*b* and data not shown). Mutant cervical LNs were 2- and 10-fold enlarged at weeks 2 and 24, respectively. Mutant mice also developed a progressive splenomegaly after weeks 6–8 (Fig. 4*b*), and the liver of 50% of mutant mice was up to 2-fold enlarged at week 20 (data not shown).

Histological examination at week 12 revealed numerous eosinophils in mutant cervical LN and spleen (Fig. 4*c*), in which an increased number of plasma cells was also seen in hematoxylin and eosin-stained sections (data not shown). A dense perivenous infiltrate rich in eosinophils, lymphocytes, and neutrophils was present in mutant liver (Fig. 4*c*). Eosinophil infiltrates were also observed to a lesser extent in mutant lung and heart at a later stage (week 20), whereas thymus examination at week 12 did not reveal any overt abnormality (data not shown).

Mice Lacking RXRα and RXRβ Activation Function 2 (AF-2) in Keratinocytes Develop an Alopecia but Not the Th2-Like Skin Inflammation and Systemic Abnormalities. To investigate whether the ligand-dependent AF-2s of RXRα and RXRβ are required to prevent the skin inflammation observed in RXR$\alpha\beta^{ep-/-}$ mutants, we crossed RXR$\alpha^{af2o/+}$ and RXR$\beta^{af2o/+}$ mice (heterozygous for the *af2*^{o} allele, which lacks the AF-2 core, refs. 18 and 19) with K14-Cre-ER$^{T2(tg/0)}$/RXR$\alpha^{L2/L2}$/RXR$\beta^{L2/L2}$ mice to generate K14-Cre-ER$^{T2(tg/0)}$/RXR$\alpha^{L2/af2o}$/RXR$\beta^{L2/af2o}$ mice. Upon Tam administration, these mice were efficiently converted to mice that, in epidermal keratinocytes, selectively expressed the RXRα and RXRβ proteins lacking AF-2 (hereafter referred to as RXR$\alpha\beta^{epaf2o}$ mice).

Like RXR$\alpha\beta^{ep-/-}$ mice, RXR$\alpha\beta^{epaf2o}$ mice developed an alopecia. Early hair loss was observed around the eye and on the dorsal skin at week 3 to week 5 (Fig. 5 *a–c*). However, unlike RXR$\alpha\beta^{ep-/-}$ mutants, RXR$\alpha\beta^{epaf2o}$ ears were neither red nor swollen (Fig. 5 *a–c Insets*), and RXR$\alpha\beta^{epaf2o}$ mice did not develop at later times the skin lesions seen in RXR$\alpha\beta^{ep-/-}$ mice (Fig. 1 and not shown). In contrast to RXR$\alpha\beta^{ep-/-}$ skin, which exhibited a dense dermal cell infiltrate and an hyperplastic epidermis at week 5, RXR$\alpha\beta^{epaf2o}$ skin showed a much weaker infiltrate, even though utriculi and dermal cysts resulting from hair follicle degeneration (11) were present in both RXR$\alpha\beta^{ep-/-}$ and RXR$\alpha\beta^{epaf2o}$ skins (Fig. 5 *d–f* and data not shown). The number of CD4$^+$ T cells and CD11c$^+$ DCs was slightly higher in RXR$\alpha\beta^{epaf2o}$ skin than in CT, but no increase in eosinophils and mast cells was observed (Fig. 5*g* and data not shown).

Like in RXR$\alpha\beta^{ep-/-}$ skin, the levels of transcripts of IFN-γ, CXCL10, and CCL20 were increased in RXR$\alpha\beta^{epaf2o}$ skin (Fig. 5*h*), whereas those of IL-4, IL-5, IL-13, IL-10, and IL-31, which are all preferentially produced by Th2 cells, were unchanged (Fig. 5*h* and data not shown), indicating that the lack of AF-2 in keratinocytic RXRα and RXRβ mainly results in a Th1-like skin inflammation. Interestingly, TSLP expression, which was highly increased in RXR$\alpha\beta^{ep-/-}$ keratinocytes, was not enhanced in RXR$\alpha\beta^{epaf2o}$ skin (Fig. 5*h*). In keeping with these transcript data, the TSLP serum level was also unchanged in RXR$\alpha\beta^{epaf2o}$ mice when compared to controls (data not shown). Moreover, serum levels of IL-5 and IgE were not elevated in RXR$\alpha\beta^{epaf2o}$ mice, and there was no eosinophilia in peripheral blood and in various organs (data not shown), indicating that RXR$\alpha\beta^{epaf2o}$ mice did not develop the systemic AD-like syndrome seen in RXR$\alpha\beta^{ep-/-}$ mice.

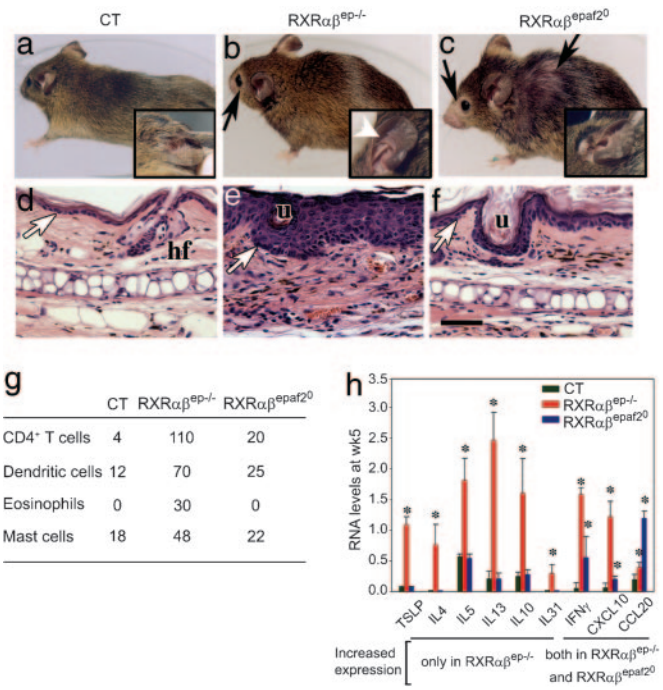

Fig. 5. RXR$\alpha\beta^{epaf2o}$ mice do not develop a skin inflammation. (*a–c*) Appearance of control (CT) (*a*), RXR$\alpha\beta^{ep-/-}$ mutant (*b*), and RXR$\alpha\beta^{epaf2o}$ mutant (*c*) at week 5. Close views of the ears are shown in *Insets*. Black arrows in *b* and *c* point to regions with hair loss, and white arrowhead in *b Inset* points to the red and swollen ear. (*d–f*) Hematoxylin/eosin staining of ear sections of CT (*d*), RXR$\alpha\beta^{ep-/-}$ mutant (e), and RXR$\alpha\beta^{epaf2o}$ mutant (*f*) at week 5. White arrows point to dermal–epidermal junction. hf, hair follicle; u, utriculi. (Scale bar, 50 μm.) (*g* and *h*) Comparison of immune cell infiltrate (*g*) and RNA levels of cytokines and chemokines (*h*) in ear skin of RXR$\alpha\beta^{ep-/-}$ and RXR$\alpha\beta^{epaf2o}$ mutant mice at week 5. The numbers in *g* represent the average counting of the corresponding cells from three microscopic fields (objective $\times$20) of ear sections. *, $P < 0.05$.

Transgenic Mice Overexpressing TSLP in Epidermal Keratinocytes Exhibit Skin and Systemic Abnormalities Similar to Those of RXR$\alpha\beta^{ep-/-}$ Mice. The close association of the early increase in TSLP expression in keratinocytes with the skin and systemic syndrome developed by RXR$\alpha\beta^{ep-/-}$ mice indicated that keratinocyte-derived TSLP could play an important role in triggering the atopic syndrome. This prompted us to generate K14-TSLP transgenic mice expressing TSLP under the control of the human K14 promoter (K14-TSLP mice). As early as 3 weeks after birth, K14-TSLP mice displayed scaly and thickened ears (Fig. 6*a*). With time, skin lesions developed on and behind the ears, on the face (Fig. 6*b*), in the neck region (Fig. 6*c*), as well as on the back (Fig. 6*d*, better seen after shaving) of these mice, which frequently exhibited a scratching behavior reflecting a skin pruritus.

Ear skin of 3-week-old K14-TSLP mice exhibited a dense dermal infiltrate (Fig. 6 *e* and *f*) consisting of numerous CD4$^+$ T cells (Fig. 6 *g* and *h*), together with CD11c$^+$ DCs and eosinophils (data not shown), whereas the number of mast cells was not increased until

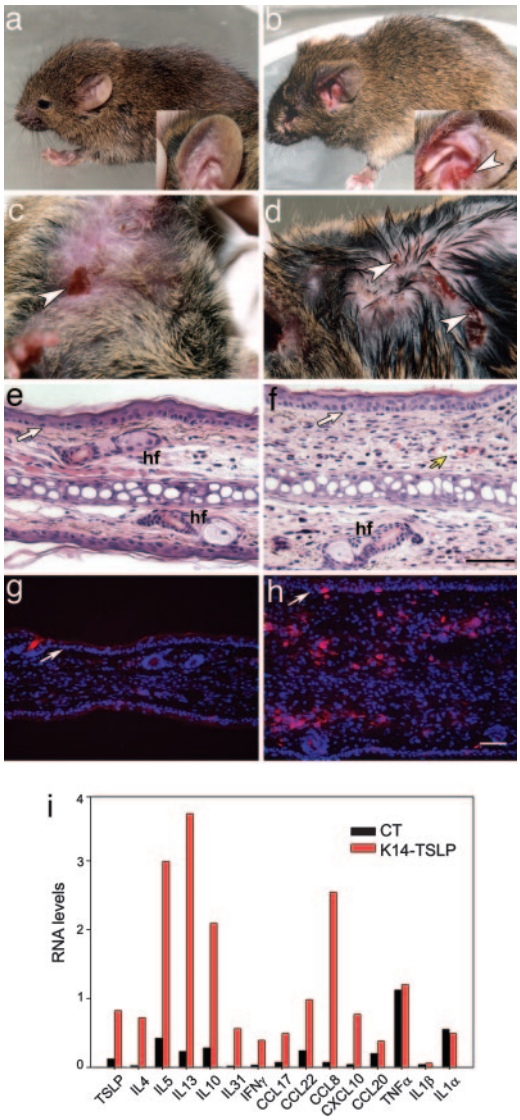

Fig. 6. K14-TSLP transgenic mice develop a chronic skin inflammation. (*a–d*) Appearance of a 3-week-old (*a*) and a 7-week-old (*b*) K14-TSLP transgenic mouse, with closer views of the ears shown in *Insets*. Photos of skin lesions exhibited by the 7-week-old K14-TSLP transgenic mouse in the neck (*c*) and on dorsal (*d*) regions were taken after shaving. White arrowheads point to lesioned skin. (*e* and *f*) Hematoxylin and eosin-stained ear sections of 3-week-old control (*e*) and K14-TSLP transgenic (*f*) mice. White arrows point to the dermal/epidermal junction. Yellow arrow points to blood vessel. hf, hair follicle. (*g* and *h*) Immunohistochemical staining of CD4 on ear sections from 3-week-old control (*g*) and K14-TSLP transgenic (*h*) mice. Red color corresponds to the staining of the antibodies, and blue corresponds to the DAPI staining of nuclei. White arrows point to dermal/epidermal junction. (Scale bars, 50 μm.) (*i*) RNA levels of cytokines and chemokines (as indicated) in ear skin of 3-week-old representative control and K14-TSLP transgenic mice.

later stages (e.g., 7 weeks old) (data not shown). Cytokine and chemokine profiles, similar to those observed in RXR$\alpha\beta^{ep-/-}$ skin, were found in ear skin of 3-week-old K14-TSLP mice, with increased levels of IL-4, IL-5, IL-13, IL-10, and IL-31 transcripts, as well as of IFN-γ and chemokines CCL17, CCL22, CXCL10, CCL8, and CCL20 transcripts, whereas there was little change in TNF-α, IL-1α, and IL-1β transcripts (Fig. 6*i*).

Moreover, K14-TSLP mice developed the systemic syndrome previously seen in RXR$\alpha\beta^{ep-/-}$ mice, i.e., elevated serum levels of IgE, IgG and IL-5, and increased number of lymphocytes and eosinophils in the blood of 5-week-old mice (Fig. 8, which is published as supporting information on the PNAS web site). K14-TSLP mice also exhibited hyperplasia of lymph nodes, spleen, and liver, with numerous eosinophils present in these tissues (Fig. 8).

Discussion

We have shown here that RXR$\alpha\beta^{ep-/-}$ mice develop a skin and systemic syndrome similar to that of human AD. Several lines of evidence strongly support the conclusion that the chronic dermatitis developed by RXR$\alpha\beta^{ep-/-}$ mice is very close to that of AD patients. First, these mice display the major clinical features of patients suffering from AD (32–34), including eczematous-like lesions, xeroxis, and pruritus. Second, in these mice, the skin inflammatory cell infiltrate is mostly composed of CD4+T and dendritic cells, associated with eosinophils and mast cells, which together are characteristic of skin lesions of AD patients (1, 20). Third, the profile of increased expression of cytokines and chemokines found in mutant inflammatory skin is typical of a Th2-type inflammation, known to be crucially involved in human AD pathogenesis (1, 24): IL-4, IL-5, IL-13, IL-10, and IL-31 are known to be Th2-type cytokines, whereas CCL17, CCL22 and CCL8 are known to preferentially chemoattract Th2 cells. Importantly, the expression of TSLP, a recently identified cytokine that was shown to be highly expressed in keratinocytes of AD patients (27), is dramatically increased in keratinocytes of mutant mice. As in chronic human AD skin lesions (35), a delayed minor component of Th1-type inflammation is also found, as indicated by an increase in Th1-type cytokines (IFN-γ and TNF-β) and chemokines (CCL10 and CCL20). Finally, most AD patients exhibit a systemic Th2-like immune syndrome similar to that found in RXR$\alpha\beta^{ep-/-}$ mice, including increased serum levels of IgE and blood eosinophilia, possibly because of IL-4 and IL-13 (switching B lymphocytes into IgE production; ref. 36) and IL-5 (promoting the growth and activation of eosinophils; ref. 37) increases.

Interestingly, our data indicate that RXRs are differentially required in keratinocytes for maintenance of the hair cycle and prevention of the occurrence of an AD-like skin and systemic syndrome. We previously reported that keratinocyte-selective ablation of RXRα is sufficient on its own to interrupt the hair cycle and to generate an alopecia, whose severity was increased by further RXRβ ablation (11, 14). Because this alopecia was similar to that observed in VDR-null (11) and VDR$^{ep-/-}$ (our unpublished results) mutants, RXR/VDR heterodimers are most probably instrumental to hair cycle maintenance (11). Here, we show clearly that, in addition, RXR AF-2 must be functional in this heterodimer, because the keratinocyte-selective inactivation of AF-2 in RXRα and RXRβ (RXR$\alpha\beta^{epaf2o}$ mutant) results in a similar alopecia. Furthermore, our finding of a Th1-like inflammatory reaction in RXR$\alpha\beta^{epaf2o}$ skin with increased expression of IFN-γ and IFN-γ-induced chemokines (CCL10 and CCL20) (38, 39), suggests that the occurrence of this alopecia could be related to an increase in IFN-γ signaling (40). In this respect, we note that there is a similar Th1-like inflammatory reaction in VDR$^{ep-/-}$ skin (our unpublished data).

On the other hand, AF-2 is clearly dispensable in the process by which RXRα and -β prevent the appearance of a Th2-like inflammatory reaction with increased expression of TSLP and Th2-type cytokines and chemokines, which strongly suggests that these cytokines and chemokines, as well as TLSP, are involved in the generation of the Th2-type AD-like skin and systemic syndrome. The identity of the heterodimeric partner(s) of RXRα and RXRβ is currently unknown, as germ-line or keratinocyte-selective ablation of retinoic acid receptors α, β, or γ, VDR, peroxisome proliferator-activated receptors α, β, or γ, liver X receptors α or β, and thyroid hormone receptors α or β did not result in the AD-like syndromes exhibited by RXR$\alpha\beta^{ep-/-}$ mutants or increased expression of Th2-type cytokines and TSLP in their skin (data not shown).

Other RXR NR partners might be involved, and/or these NRs could be functionally redundant.

Several lines of evidence strongly support the conclusion that TSLP plays a key role in the chain of events that generate the Th2-type skin and systemic atopic syndrome. First, among the various cytokines aberrantly expressed in RXR$\alpha\beta^{ep-/-}$ mutants, TLSP is the earliest to be strongly overproduced in basal keratinocytes (Fig. 3), and moreover, its up-regulation is tightly correlated with the occurrence of the atopic skin and systemic syndrome (TSLP is overproduced in RXR$\alpha\beta^{ep-/-}$ mice, but not in RXR$\alpha\beta^{epaf2o}$ mice). Furthermore, the same functional redundancy exists between RXRα and RXRβ for the presence of increased levels of TLSP transcripts in keratinocytes and TSLP proteins in serum (Fig. 9, which is published as supporting information on the PNAS web site) and for the occurrence of the AD-like skin and systemic syndrome. Finally, and most importantly, expressing TSLP in epidermal keratinocytes of transgenic mice generates AD-like skin and systemic abnormalities closely mimicking those seen in RXR$\alpha\beta^{ep-/-}$ mice, thus unequivocally demonstrating that TSLP produced in keratinocytes is the initiating cytokine at the top of a chain of immunological events that lead to the atopic syndrome in RXR$\alpha\beta^{ep-/-}$ mutants.

In fact, TSLP may very well play a similar role in AD patients, because human TSLP has been recently found to be produced by keratinocytes from AD patients, but not from human normal skin or patients with nickel-induced contact dermatitis (a Th1-like inflammation) (27, 41). Moreover, *in vitro* studies have shown that human TSLP activates dendritic cells, which can induce differentiation of allogenic proallergic Th2 cells (41) as well as homeostatic proliferation of autologous $CD4^+$ T cells (42). Whether similar mechanisms mediate the effect of TSLP overproduced in mouse and human keratinocytes to trigger the AD skin and systemic immune reactions remains to be investigated.

It remains also to be seen how the overproduction of TSLP is triggered in human skin of AD patients and to what extent a dysregulation of NR pathways involving RXRs could be implicated in the pathogenesis of AD. That TSLP expression in RXR$\alpha\beta^{ep-/-}$ could be caused by the relief of a transcriptional repression is suggested by the dispensability of the ligand-dependent RXR activation function AF-2. In this respect, we also note that (*i*) putative NR response elements are present in the upstream region of the mouse and human TLSP promoters (Fig. 10, which is published as supporting information on the PNAS web site) and (*ii*) such a repression is unlikely to be exerted by RXR homodimers, as it is not relieved by administration of a RXR agonist (data not shown). In any event, our present data point to a key role of epidermal keratinocytes in the initiation of atopic dermatitis and its systemic manifestations. Whether epidermal-produced TSLP could be instrumental to the pathogenesis of other atopic diseases (e.g., asthma, ref. 34) and Th2-mediated diseases (e.g., hypereosinophilic syndrome, ref. 43) remains also to be examined. Transgenic mice overexpressing TSLP in different tissues, as well as tissue-selective conditional somatic mutations of the TSLP gene, should offer new useful models (44, 45) for investigating further the pathogenesis of atopic diseases and testing possible therapies.

We thank P. Hener for excellent technical assistance and M. Duval for mouse care. We are grateful to the staff of the mouse, histopathology, hematology, and transgenic facilities of the Institut Clinique de la souris (ICS) and Institut de Génétique et de Biologie Moléculaire et Cellulaire (IGBMC) for their kind help, and the secretariat for typing the manuscript. We also thank B. Mascrez (ICS) for RXR$\alpha^{af20/+}$ and RXR$\beta^{af20/+}$ mice, and Dr. B. Cribier (Hôpitaux Universitaires de Strasbourg) and S. Chan (IGBMC) for useful discussion. This work was supported by funds from the Centre National de la Recherche Scientifique, the Institut National de la Santé et de la Recherche Médicale, the Collège de France, the Hôpital Universitaire de Strasbourg, the Association pour la Recherche sur le Cancer, the Fondation pour la Recherche Médicale, and the Human Frontier Science Program, and the Ministère de la Recherche.

1. Leung, D. Y., Boguniewicz, M., Howell, M. D., Nomura, I. & Hamid, Q. A. (2004) *J. Clin. Invest.* **113,** 651–657.
2. Leung, D. Y., Jain, N. & Leo, H. L. (2003) *Curr. Opin. Immunol.* **15,** 634–638.
3. Esche, C., de Benedetto, A. & Beck, L. A. (2004) *Curr. Allergy Asthma Rep.* **4,** 276–284.
4. Mangelsdorf, D. J., Thummel, C., Beato, M., Herrlich, P., Schutz, G., Umesono, K., Blumberg, B., Kastner, P., Mark, M., Chambon, P., *et al.* (1995) *Cell* **83,** 835–839.
5. Laudet, V. & Gronemeyer, H. (2002) *The Nuclear Receptor: Facts Book* (Academic, San Diego).
6. Kastner, P., Mark, M. & Chambon, P. (1995) *Cell* **83,** 859–869.
7. Zhang, X. & Young, H. A. (2002) *Int. Immunopharmacol.* **2,** 1029–1044.
8. Winoto, A. & Littman, D. R. (2002) *Cell* **109,** Suppl., S57–S66.
9. Chambon, P. (1996) *FASEB J.* **10,** 940–954.
10. Chambon, P. (2005) *Mol. Endocrinol.* **19,** 1418–1428.
11. Li, M., Indra, A. K., Warot, X., Brocard, J., Messaddeq, N., Kato, S., Metzger, D. & Chambon, P. (2000) *Nature* **407,** 633–636.
12. Fisher, G. J. & Voorhees, J. J. (1996) *FASEB J.* **10,** 1002–1013.
13. Chapellier, B., Mark, M., Messaddeq, N., Calleja, C., Warot, X., Brocard, J., Gerard, C., Li, M., Metzger, D., Ghyselinck, N. B. & Chambon, P. (2002) *EMBO J.* **21,** 3402–3413.
14. Li, M., Chiba, H., Warot, X., Messaddeq, N., Gerard, C., Chambon, P. & Metzger, D. (2001) *Development (Cambridge, U.K.)* **128,** 675–688.
15. Kastner, P., Mark, M., Leid, M., Gansmuller, A., Chin, W., Grondona, J. M., Decimo, D., Krezel, W., Dierich, A. & Chambon, P. (1996) *Genes Dev.* **10,** 80–92.
16. Metzger, D., Indra, A. K., Li, M., Chapellier, B., Calleja, C., Ghyselinck, N. B. & Chambon, P. (2003) *Methods Enzymol.* **364,** 379–408.
17. Metzger, D., Li, M. & Chambon, P. (2004) *Methods Mol. Biol.* **289,** 329–340.
18. Mascrez, B., Mark, M., Dierich, A., Ghyselinck, N. B., Kastner, P. & Chambon, P. (1998) *Development (Cambridge, U.K.)* **125,** 4691–4707.
19. Mascrez, B., Ghyselinck, N. B., Watanabe, M., Annicotte, J. S., Chambon, P., Auwerx, J. & Mark, M. (2004) *EMBO Rep.* **5,** 285–290.
20. Thestrup-Pedersen, K. (1997) in *Skin Immune System*, ed. Bos, J. D. (CRC, Boca Raton, FL), pp. 497–507.
21. Lucey, D. R., Clerici, M. & Shearer, G. M. (1996) *Clin. Microbiol. Rev.* **9,** 532–562.
22. Abbas, A. K., Murphy, K. M. & Sher, A. (1996) *Nature* **383,** 787–793.
23. O'Garra, A. (1998) *Immunity* **8,** 275–283.
24. Dillon, S. R., Sprecher, C., Hammond, A., Bilsborough, J., Rosenfeld-Franklin, M., Presnell, S. R., Haugen, H. S., Maurer, M., Harder, B., Johnston, J., *et al.* (2004) *Nat. Immunol.* **5,** 752–760.
25. Schon, M. P., Zollner, T. M. & Boehncke, W. H. (2003) *J. Invest. Dermatol.* **121,** 951–962.
26. Schutyser, E., Struyf, S. & Van Damme, J. (2003) *Cytokine Growth Factor Rev.* **14,** 409–426.
27. Soumelis, V. & Liu, Y. J. (2004) *Springer Semin. Immunopathol.* **25,** 325–333.
28. Sims, J. E., Williams, D. E., Morrissey, P. J., Garka, K., Foxworthe, D., Price, V., Friend, S. L., Farr, A., Bedell, M. A., Jenkins, N. A., *et al.* (2000) *J. Exp. Med.* **192,** 671–680.
29. Stevens, T. L., Bossie, A., Sanders, V. M., Fernandez-Botran, R., Coffman, R. L., Mosmann, T. R. & Vitetta, E. S. (1988) *Nature* **334,** 255–258.
30. Baatjes, A. J., Sehmi, R., Saito, H., Cyr, M. M., Dorman, S. C., Inman, M. D., O'Byrne, P. M. & Denburg, J. A. (2002) *Pharmacol. Ther.* **95,** 63–72.
31. Simon, H. U., Plotz, S. G., Dummer, R. & Blaser, K. (1999) *N. Engl. J. Med.* **341,** 1112–1120.
32. Leung, D. Y. & Bieber, T. (2003) *Lancet* **361,** 151–160.
33. Hanifin, J. M. a. R., G. (1980) *Acta Dermatovener (Stockholm)*, Suppl. 92, 44–47.
34. Spergel, J. M. & Paller, A. S. (2003) *J. Allergy Clin. Immunol.* **112,** S118–27.
35. Grewe, M., Bruijnzeel-Koomen, C. A., Schopf, E., Thepen, T., Langeveld-Wildschut, A. G., Ruzicka, T. & Krutmann, J. (1998) *Immunol. Today* **19,** 359–361.
36. Jelinek, D. F. (2000) *Ann. Allergy Asthma Immunol.* **84,** 375–385; quiz 385–387.
37. Lopez, A. F., Sanderson, C. J., Gamble, J. R., Campbell, H. D., Young, I. G. & Vadas, M. A. (1988) *J. Exp. Med.* **167,** 219–224.
38. Luster, A. D., Unkeless, J. C. & Ravetch, J. V. (1985) *Nature* **315,** 672–676.
39. Nakayama, T., Fujisawa, R., Yamada, H., Horikawa, T., Kawasaki, H., Hieshima, K., Izawa, D., Fujiie, S., Tezuka, T. & Yoshie, O. (2001) *Int. Immunol.* **13,** 95–103.
40. Ito, T., Ito, N., Saathoff, M., Bettermann, A., Takigawa, M. & Paus, R. (2005) *Br. J. Dermatol.* **152,** 623–631.
41. Soumelis, V., Reche, P. A., Kanzler, H., Yuan, W., Edward, G., Homey, B., Gilliet, M., Ho, S., Antonenko, S., Lauerma, A., *et al.* (2002) *Nat. Immunol.* **3,** 673–680.
42. Watanabe, N., Hanabuchi, S., Soumelis, V., Yuan, W., Ho, S., De Waal Malefyt, R. & Liu, Y. J. (2004) *Nat. Immunol.* **5,** 426–434.
43. Roufosse, F., Cogan, E. & Goldman, M. (2003) *Annu. Rev. Med.* **54,** 169–184.
44. Shiohara, T., Hayakawa, J. & Mizukawa, Y. (2004) *J. Dermatol. Sci.* **36,** 1–9.
45. Gutermuth, J., Ollert, M., Ring, J., Behrendt, H. & Jakob, T. (2004) *Int. Arch. Allergy Immunol.* **135,** 262–276.